J. Fluid Mech. (1996), *vol.* 309, *pp.* 93–111

Resonant interaction of a linear array of supersonic rectangular jets: an experimental study

By GANESH RAMAN[1] AND RAY TAGHAVI[2]

[1] NYMA Inc., Experimental Fluid Dynamics Section, NASA Lewis Research Center Group, Brookpark, OH 44142, USA

[2] Department of Aerospace Engineering, University of Kansas, Lawrence, KS 66045, USA

(Received 26 October 1994 and in revised form 9 October 1995)

This paper examines a supersonic multi-jet interaction problem that we believe is likely to be important for mixing enhancement and noise reduction in supersonic mixer–ejector nozzles. We demonstrate that it is possible to synchronize the screech instability of four rectangular jets by precisely adjusting the inter-jet spacing. Our experimental data agree with a theory that assumes that the phase-locking of adjacent jets occurs through a coupling at the jet lip. Although synchronization does not change the frequency of the screech tone, its amplitude is augmented. The synchronized multi-jets exhibit higher spreading than the unsynchronized jets, with the single jet spreading the least. We compare the near-field noise of the four jets with synchronized screech to the noise of the sum of four jets operated individually. Our noise measurements reveal that the more rapid mixing of the synchronized multi-jets causes the peak jet noise source to move upstream and to radiate noise at larger angles to the flow direction. Based on our results, we have grounds to believe that screech synchronization is advantageous for noise reduction internal to a mixer–ejector nozzle, since the noise can now be suppressed by a shorter acoustically lined ejector.

1. Introduction

1.1. *Motivation for the present work*

Enhanced mixing of supersonic rectangular jets is of current interest to the High-Speed Research community. Efforts are focused on meeting the noise requirements for the next-generation supersonic airplane. In order to meet the noise goal, researchers have suggested several types of mixer–ejector nozzle configurations. By enhancing the mixing and/or changing the directivity of its sound, we can considerably shorten ejector length and yet obtain the same noise suppression. While there are some engineering data on these mixer–ejector nozzle configurations, there is not enough information on simpler configurations that could aid in the fundamental understanding of such flows. Morris (1990) emphasized the need for further experimental data on multiple supersonic jets including data on the modification of the growth rate of the jet mixing layer, mean flow contours in the merged jet region, and measurements of the entrained flow between the jets. The need for such data is crucial because there is neither a stability analysis, nor a numerical simulation of multiple supersonic shock-containing jets. Providing such information is one of our objectives.

The present work also studies the rectangular nozzle as an element of a lobed mixer–ejector nozzle. We emphasize simple geometries that could be used internal to a shroud, which leads to a focus on the mixing and the near-field acoustics. More specifically, our aim is to study the flow and noise of multi-jets under conditions of

screech synchronization. The present work demonstrates that it is possible to synchronize the flapping screech instability mode in a linear array of four jets, which yields enhanced mixing. The increased mixing rate of the jets moves the jet noise source upstream, providing a longer propagation length for an acoustic lining to reduce the internal mixing noise.

1.2. *Review of previous work*

Jets operated off-design are known to produce an intense tone known as 'jet screech'. Screeching jets have now been studied by several researchers including Powell (1953), Lassiter & Hubbard (1954), Hammitt (1961), Davies & Oldfield (1962*a*, *b*), Glass (1968), Krothapalli *et al.* (1986), Gutmark, Schadow & Bicker (1990), and an excellent summary was provided by Tam (1991). It is now well recognized that the screech tone is created by growing coherent disturbances in the jet interacting with the shocks. The tone then propagates upstream (as feedback) to the jet exit and excites instabilities in the jet, thus closing the resonant loop. It is also well established (Glass 1968) that screeching jets have spread rates that are greater than their non-screeching counterparts. It is, therefore, attractive to use a natural excitation source such as jet screech, that uses no external power, for jet mixing enhancement and noise control.

It is interesting to note that the response of a jet to screech is very similar to its response to an edgetone. Edgetones have been studied extensively (Powell 1961; Karamcheti *et al.* 1969; Rockwell 1983; Crighton 1992), and researchers have also focused on the mixing enhancement of a jet excited by an edgetone (Krothapalli *et al.* 1983; Rice & Raman 1993; Raman & Rice 1995). Krothapalli *et al.* (1983) reported mixing enhancement in a multi-jet arrangement when a wedge was inserted into the middle of one of the jets, downstream of the nozzle. All five subsonic jets responded with enhanced mixing. However, this interesting observation was not pursued further.

Most published twin-jet work has focused on round jets. The acoustical properties, including the shielding effect of heated twin jets, were studied by Kantola (1981). The dynamic inter-nozzle pressure loads and resonance characteristics of a pair of circular jets were studied by Seiner, Manning & Ponton (1988). The manner in which the resonant coupling depended on the inter-nozzle spacing was investigated by Wlezien (1989). In addition, Morris (1990) presented calculations for the characteristics of instability waves in the initial mixing region of resonantly interacting twin circular supersonic jets. There is, however, only a limited amount of data on a linear array of rectangular jets: Krothapalli, Baganoff & Karamcheti (1979); Chandrashekara, Krothapalli & Baganoff (1984); Marsters (1980); Taghavi & Raman (1994). Moreover, to our knowledge a detailed description of multi-jets with synchronized screech is unavailable in the published literature.

The noise of a supersonic shock-containing jet consists of tonal and non-tonal (broadband) components. The tonal components include the screech tone and its harmonics, whereas the non-tonal components include shock-associated broadband noise and jet mixing noise. Screech is produced by a strong interaction between the advecting coherent structures and the standing shock waves. A weak interaction between the structures and the shocks produces broadband shock-associated noise. The relationship between shock-associated broadband noise and screech tones was discussed by Tam, Seiner & Yu (1986). Jet mixing noise caused by large-scale coherent structures in the jet was described by Lighthill (1952, 1954), Lush (1971), and Crighton (1974), and an impressive summary was provided by Lilley (1991).

Although several studies (e.g. Moore 1977; Ffowcs Williams & Kempton 1978; Crighton 1981; Mankbadi & Liu 1984; Bridges & Hussain 1992) have addressed the relationship between large-scale structures and noise of subsonic jets, the connection

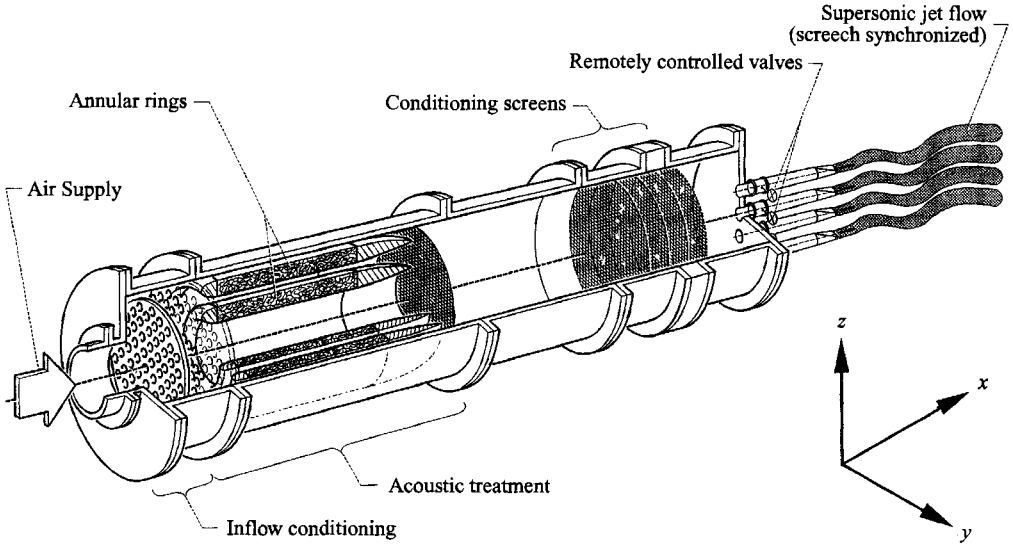

FIGURE 1. Schematic of the supersonic jet facility.

between the two appears incomplete, possibly owing to subsonically advecting coherent structures not being efficient noise producers. In contrast, despite the varied and complex nature of supersonic jet noise, there is a unique connection between each noise component (jet mixing noise, screech and shock-associated broadband noise) and the large-scale structures (Tam 1991, 1995).

In the present work, we attempt to document the tonal noise components from supersonic multi-jets with synchronized screech. In addition, we compare the jet mixing noise and shock-associated broadband noise from the synchronized supersonic multi-jets to that from the sum of the four jets run individually.

2. Apparatus and instrumentation

2.1. *Jet facility*

The experiments were carried out at the NASA Lewis Research Center Jet Facility. Figure 1 shows a schematic of the jet facility. The 76 cm diameter plenum tank was supplied with compressed air at pressures up to 875 kPa (125 P.s.i.g.) at 26.7 °C (80 °F). After passing through a filter that removes any dirt or dust, the air entered the plenum axially where it was laterally distributed by a perforated plate and a screen. Two circumferential splitter rings that contained acoustic treatment (kevlar) removed upstream valve noise. The flow was further conditioned by two 50-mesh screens before exiting into the room through the nozzles.

Figure 2 shows the multi-nozzle set up. The flow from each nozzle could be controlled independently using remotely controlled valves. The spacing between adjacent nozzles could be changed using the positioning apparatus shown in the schematic (figure 2). An automatic feedback control system was used to maintain constant air-supply conditions. The control system could restrict pressure variations during each run to within 0.2%. Such precise control was essential for this experiment since the phase-locking between the four jets, which depended on the acoustic feedback from screech sources, was extremely sensitive to changes in operating conditions.

The nozzle contour and dimensions are depicted in figure 3. Each nozzle included a

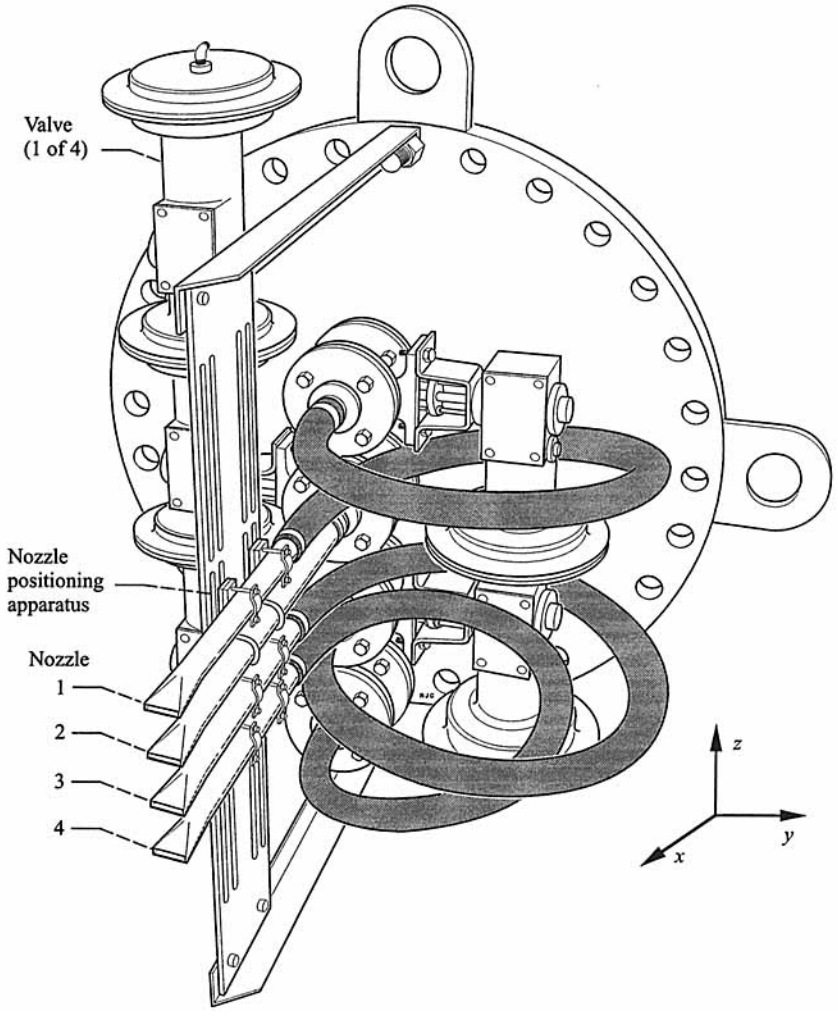

FIGURE 2. Multi-nozzle experimental apparatus.

circular-to-rectangular transition section, and a converging nozzle contour, all integrated into one piece. The nozzles, the probe traversing mechanism, and other reflective surfaces in the near field were covered with two layers of acoustically absorbent open-cell polyurethane foam (0.635 cm thick uncompressed). The idea was to minimize strong reflections from the nozzles and plenum. The material is known to be very effective in absorbing incident sound in the frequency range 1000–25000 Hz (with several layers, lower frequencies can also be absorbed). Note that for the operating conditions used in the present work, the screech tone frequencies ranged from 5344 Hz (for a fully expanded Mach number, $M_j = 1.75$) to 12768 Hz ($M_j = 1.25$). The jet mixing noise and shock-associated broadband noise are also in the range where the acoustically absorbent material is effective.

2.2. *Measurement techniques*

Measurements were made using a Pitot probe (o.d. of 0.8 mm) that traversed the entire flow field of the multi-jets. The probe was positioned by a three-dimensional traversing mechanism and controlled by computer. The Pitot probe was connected to a pressure

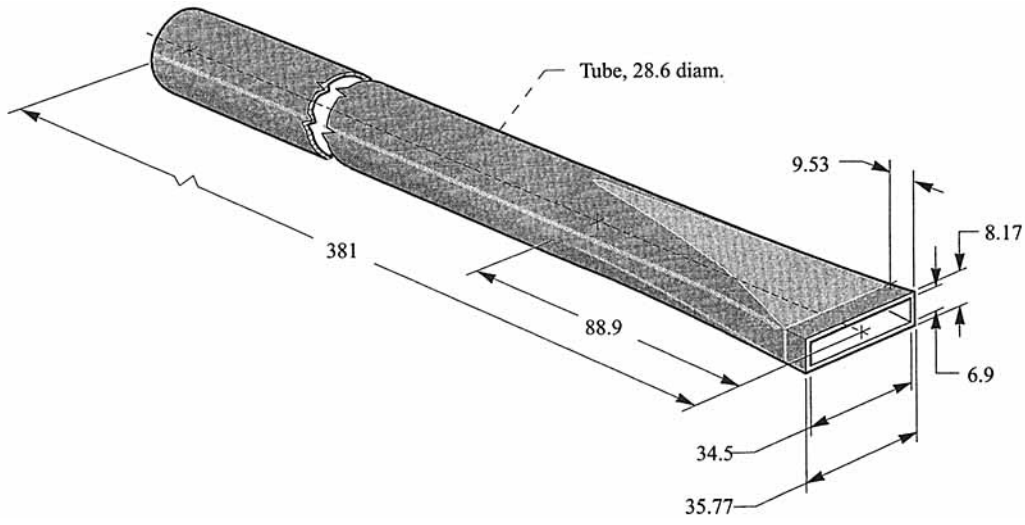

FIGURE 3. Rectangular nozzle with dimensions in mm.

transducer by a Tygon tube (0.8 mm i.d.). Three different pressure transducers, having a maximum range of 350 kPa (50 P.s.i.g.), 105 kPa (15 P.s.i.g.), and 35 kPa (5 P.s.i.g.), were used for the measurements. The centreline pressure at every axial station was used as a guide to select the transducer of an appropriate range for maximum sensitivity. The location of the flow measurement planes is depicted in figure 4(*a*).

The acoustic measurements were made using 0.64 cm (1/4 in.) diameter B & K microphones mounted under each nozzle and on the three-dimensional traversing mechanism for the near field noise surveys. The B & K microphones were omnidirectional within ± 1 dB up to 10 kHz and within ± 3 dB up to 20 kHz. The microphones were calibrated using a B & K pistonphone calibrator, with corrections for day-to-day changes in atmospheric pressure. The sound pressure levels reported in this paper are in dB relative to 20 μPa.

For the microphone measurements outside the jet, we were careful to avoid the very near field that is dominated by the potential field of the coherent hydrodynamic modes in the jet. The measurements made outside the jet are thus dominated by the acoustic field. The noise measurement planes are shown in figure 4(*b*).

3. Jet spacing for screech synchronization

Figure 5 shows schlieren photographs of the edge view (smaller dimension) of supersonic jets at various fully expanded jet Mach numbers. The spark schlieren photographs reveal the shock cells, the large-scale coherent structures, and the sinuous flapping instability of the jet. The shock-cell spacings obtained from schlieren photographs compared well with those obtained using a dual-cone static pressure probe. The static pressure probe was constructed based on the design of Pinckney (1975), and was similar to the probe used by Norum & Seiner (1982).

The average shock-cell spacings (L_s/h; h is the narrow dimension of the nozzle) obtained using the static pressure probe are given in table 1 and will be used in constructing a theoretical model for jet synchronization. For the M_j range from 1.25 to 1.75, the measured shock-cell spacings agreed with Tam's (1988) theory. The schlieren photos also indicate that the screech source moves from the third shock to the

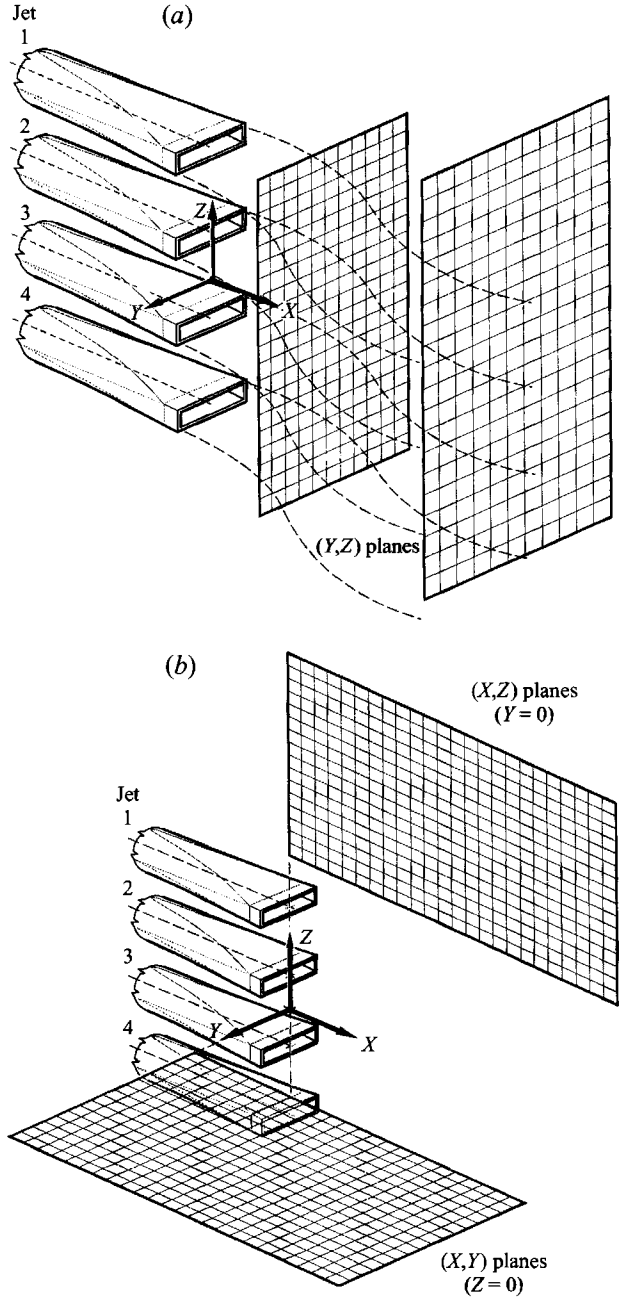

FIGURE 4. Measurement planes for (*a*) the flow field and (*b*) the near-field noise.

fourth as one goes from $M_j = 1.5$ to 1.6. This observation is also incorporated into the model to be described later in this section. Other features of single supersonic rectangular jets are described in Raman & Rice (1994) and will not be reiterated here.

Figure 6 shows a schematic of the jet spacing for screech synchronization. Following ideas of Powell (1953), Poldervaart, Vink & Wijnands (1968) and Poldervaart Wijnands & Bronkhurst (1973) we can determine the spacing for synchronization by assuming that each jet is influenced only by its immediate neighbours. The effect of the

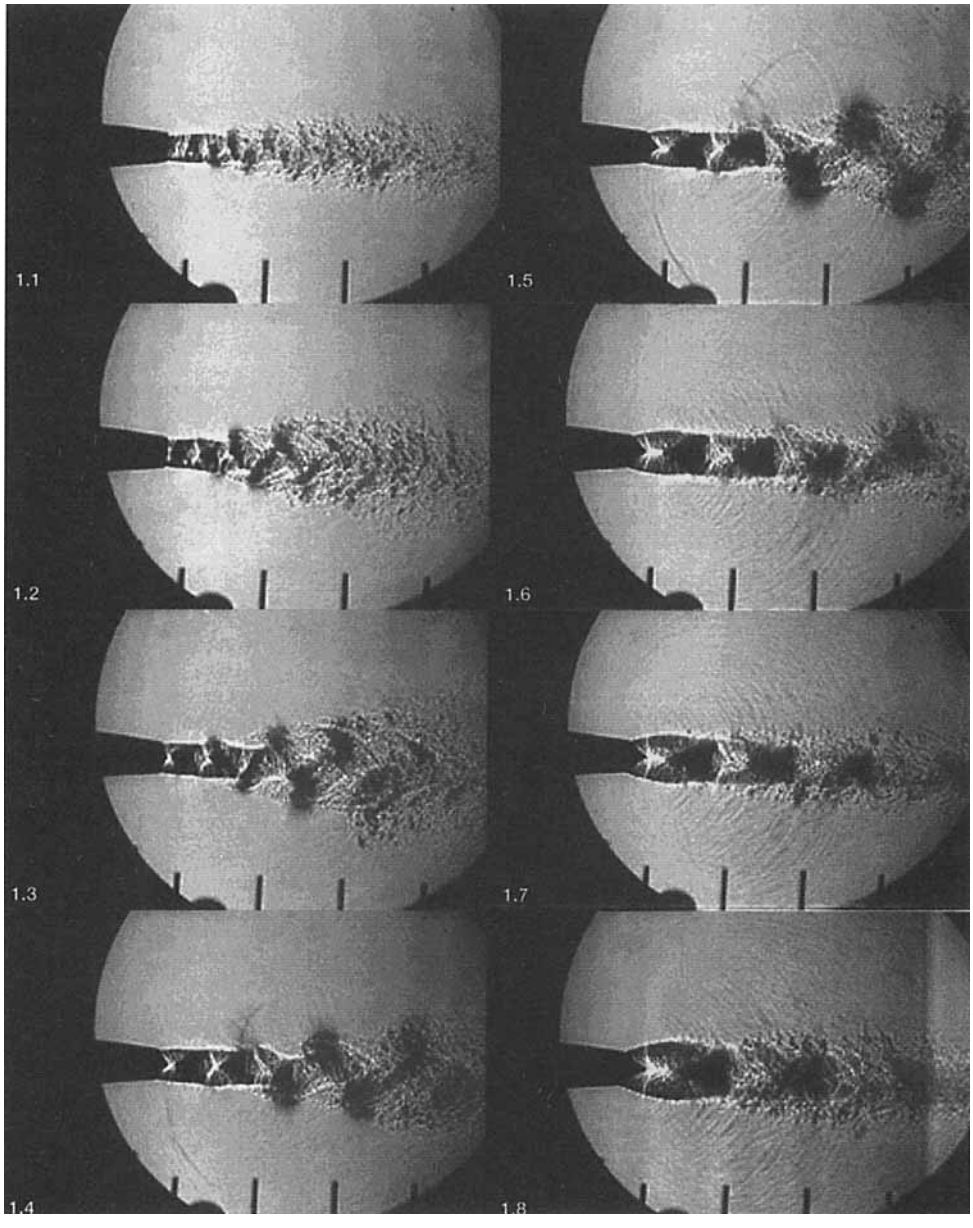

FIGURE 5. Spark schlieren photographs of the narrow dimension of underexpanded rectangular jets at the various M_j values shown on the figure.

screech tone from the other jets is assumed to be insignificant owing to the shielding effect of the neighbour jet. Experimental data were obtained by operating only jet 1 (see figure 6) and measuring the relative phase at the screech frequency between a microphone located at s1 and another that was moved from s1 to s2. The signal from the stationary microphone represents the screech signal of jet 1 that propagated upstream (as feedback) by path q to the exit of jet 1, whereas the traversing microphone measurement represents the signal obtained by a longer feedback path. A phase difference of 180° is required between microphones at s1 and s2 for synchronization of

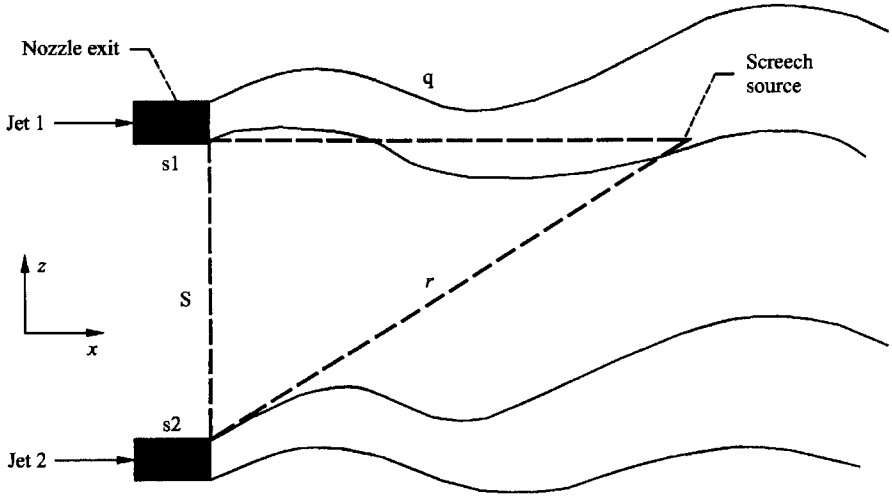

FIGURE 6. Schematic of jet spacing required for screech synchronization.

M_j	f (Hz)	λ/h	kh	L_s/h (average)	q_s/h	s/h (theory)	s/h (expt.)
1.25	12192	4.08	1.530	1.343	4.029	4.53	4.0
1.35	10200	4.88	1.287	1.849	5.547	5.76	5.5
1.45	8512	5.84	1.076	2.270	6.81	6.99	7.5
1.55	7136	6.97	0.900	2.766	11.06	9.51	10.0
1.65	5952	8.36	0.751	3.520	14.08	11.66	11.5
1.75	5280	9.43	0.667	4.311	17.24	13.62	13.7

TABLE 1. Calculation of jet spacing for screech synchronization

the screech from adjacent jets (i.e. microphones located at symmetric locations on two adjacent nozzles would sense a phase difference of zero). The inter-jet phase difference from the above measurement for jets at various Mach numbers is plotted versus a dimensionless distance (z/h) in figure 7(a). Note that jets at a higher Mach number require a larger inter-jet spacing for screech synchronization since the acoustic wavelength of screech increases with M_j.

Figure 7(a) also shows the existence of a region where the phase does not change, that we refer to as the 'null' region. This null region is seen to increase with the fully expanded jet Mach number, M_j. The existence of the null region and its growth with an increase in M_j can be reconciled as follows. As M_j increases, the screech source moves downstream, and, therefore, the wavefronts arriving at the nozzle exit plane would be flatter in the near nozzle region as M_j increases.

We model the phase variation and the null region by considering the screech source to be represented by a simple source. The acoustic pressure at any distance r (see figure 6) from the source can be assumed to be of the form

$$P(r) = \frac{A\,\mathrm{e}^{\mathrm{i}kr}}{r}, \tag{1}$$

where A represents the amplitude and k represents the wavenumber ($k = 2\pi/\lambda$; λ is the screech wavelength).

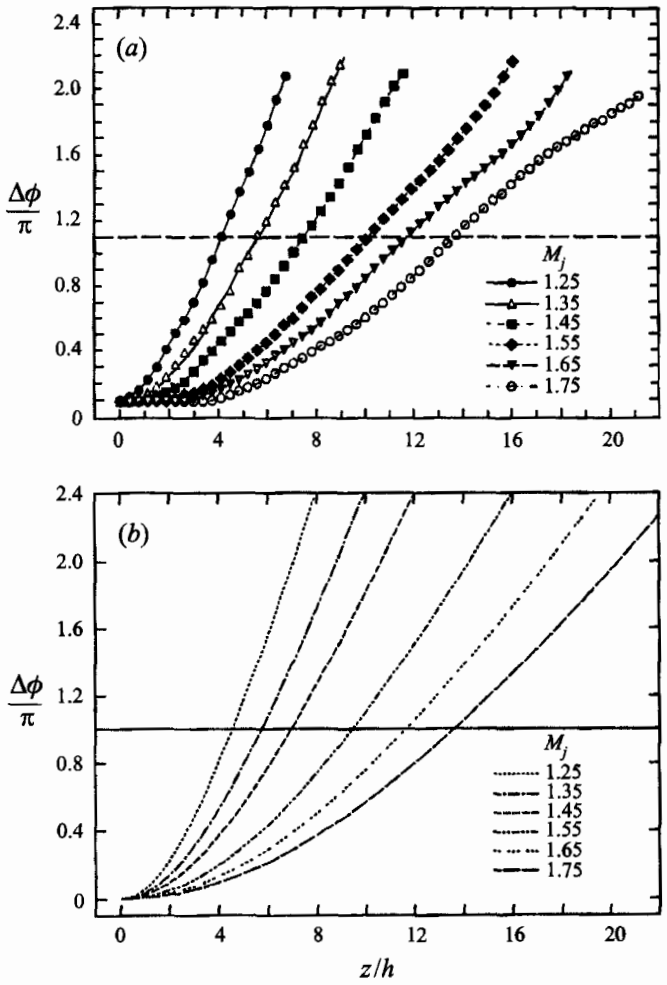

FIGURE 7. (*a*) Measured and (*b*) calculated (using (4)) relative phase in the inter-nozzle region for various fully expanded jet Mach numbers.

The phase at any point r is

$$\phi = kr; \tag{2}$$

referring to figure 6

$$\phi = k(q^2+z^2)^{1/2}, \tag{3}$$

where z is a variable distance between s1 and s2.

The phase difference between a microphone at s1 and another that is moved in the z-direction from s1 to s2 is

$$\Delta\phi = k[(q^2+z^2)^{1/2}-q]. \tag{4}$$

Note that q is the distance from the jet exit to the screech source. Both q and k depend on the jet's Mach number.

The best agreement between the model and the experimental data is obtained if it is assumed that the screech source is located at the third shock for $M_j = 1.25$, 1.35, and 1.45, and at the fourth shock for $M_j = 1.55$, 1.65, and 1.75. The theoretical model for the phase in the inter-jet region is shown in figure 7(*b*) (also see table 1). The theory is seen to model the null region and the phase change in the inter-jet region reasonably

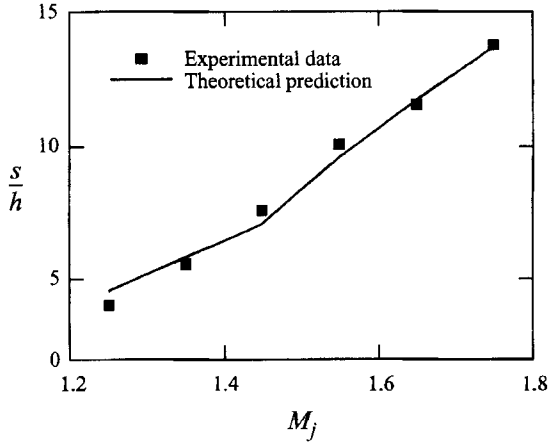

FIGURE 8. Comparison of the experimental and theoretical nozzle spacings required for screech synchronization.

well. The resemblance between the theoretical (figure 7*b*) and experimental (figure 7*a*) curves clarifies that for the jet operating conditions of the present work, the flatness of the wavefronts produces the null region. It should be noted that the model presented here is an improvement over that presented in our earlier conference paper (Raman & Taghavi 1995).

Our assumption of the screech source location is substantiated by the spark schlieren photographs shown in figure 5. In the schlieren photos the apparent screech source moves from the third shock to the fourth shock as one goes from $M_j = 1.5$ to 1.6. The theoretical inter-jet spacing required for screech synchronization normalized by the narrow dimension of the jet (h) is compared to experimental data in figure 8. Note that s/h in figure 8 is the z/h value where $\Delta\phi/\pi = 1$ for various M_j in figure 7. Note also that the theory includes the null region which is a part of the physics of the resonance phenomenon.

Following the above experiments on a single jet, we conducted an experiment on four rectangular jets. The inter-nozzle spacing was very close ($s/h = 8.16$, at $M_j = 1.6$) to that determined by the theory and by the single-jet experiments. As stated earlier, our theory assumed that the synchronization most likely occurred due to mechanisms at the jet lip. The data presented in this section show that the inter-jet spacing for screech synchronization was so large ($s/h = 8.16$ at $M_j = 1.6$) that the potential fields of neighbouring jets could not possibly have influenced each other. In addition, the synchronization is very sensitive to changes in spacing (s/h) – an observation that excludes the potential field coupling as the possible cause of screech synchronization. It follows that in the absence of any other probable mechanism, phase-locking through mechanisms at the jet lip is most likely.

4. Mean flow field of synchronized and unsynchronized jets

Since we wanted to study how synchronization affects the enhanced mixing of supersonic jets, we acquired mean flow data for three multi-jet operating conditions: (*a*) $M_j = 1.4$, $s/h = 5$; (*b*) $M_j = 1.6$, $s/h = 5$; (*c*) $M_j = 1.6$, $s/h = 8$. Cases (*a*) and (*b*) have the same inter-jet spacing but different Mach numbers, whereas cases (*b*) and (*c*) have the same Mach number but different inter-jet spacings. For case (*a*) two out of

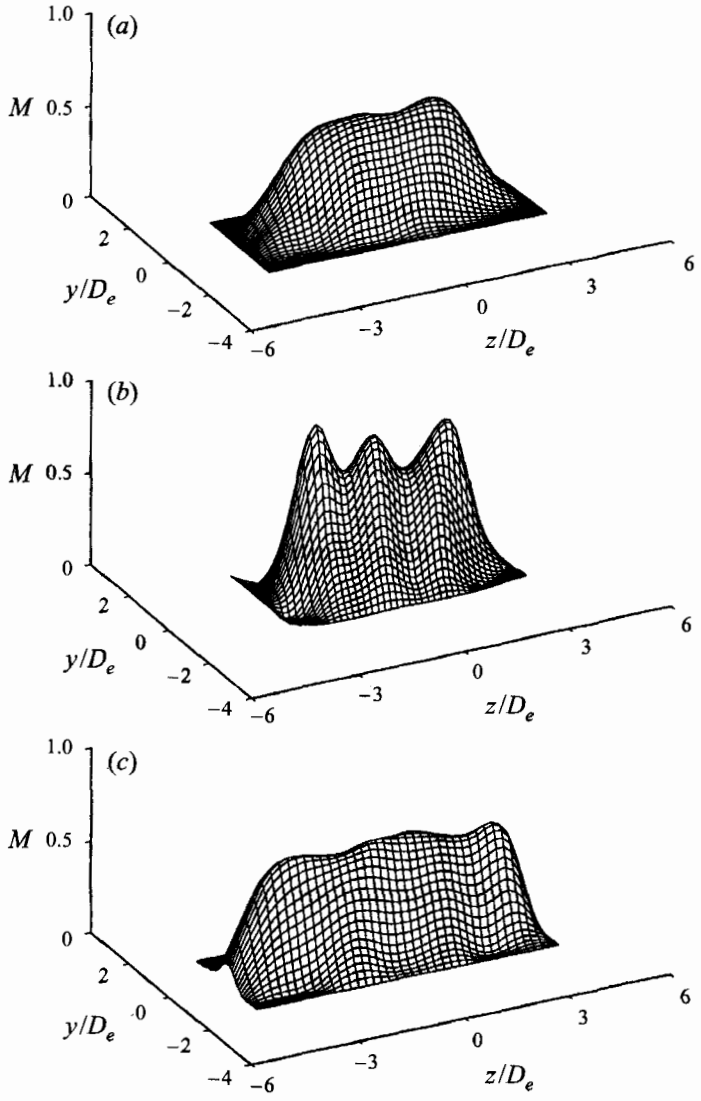

FIGURE 9. Mean flow-field data at $x/D_e = 7$ in the (y, z)-plane. (*a*) $M_j = 1.4$, $s/h = 5$; two out of four jets were synchronized. (*b*) $M_j = 1.6$, $s/h = 5$; none of the four jets was synchronized. (*c*) $M_j = 1.6$, $s/h = 8$; all four jets were synchronized.

four jets were synchronized. In contrast, for case (*b*), none of the four jets was synchronized. Finally, in case (*c*), all four jets were synchronized. Note that in case (*a*) the two synchronized jets are those located at the bottom (jets 3 and 4 in figure 2). Case (*a*) was obtained by first synchronizing all four jets, and then displacing the top two jets very slightly to make them unsynchronize. Since the synchronization is very sensitive to inter-jet spacing, the unsynchronization was easily achieved.

Pitot probe measurements were made on the (Y, Z) plane at several X/D_e stations ($D_e = (4A_0/\pi)^{1/2}$ and A_0 is the total exit area of the four jets). The Mach number data shown in figure 9 at one axial station ($x/D_e = 7$) were obtained from the Pitot tube data assuming that the local static pressure can be approximated by ambient pressure.

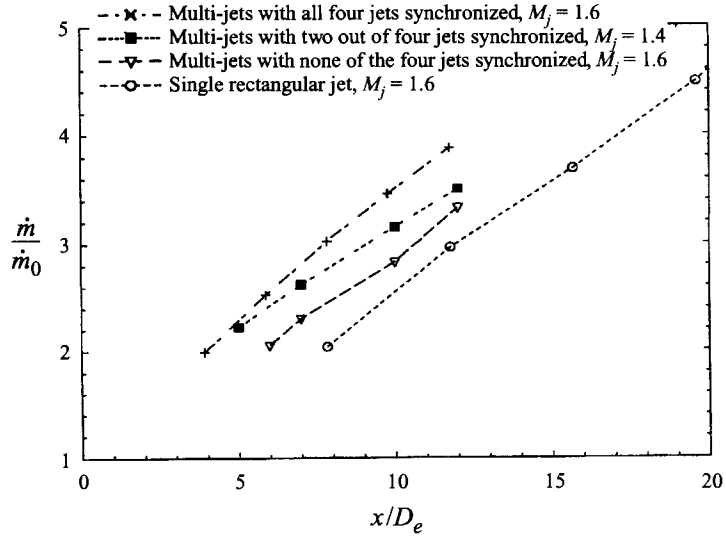

FIGURE 10. Variation of the integrated mass-flux ratio with downstream distance.

Such an approximation is reasonable for stations beyond the shock structures and supersonic regions of the jet.

From the surface plots of figure 9, it appears that case (*c*) where all four jets are synchronized has the highest jet spread, indicated by the merging of the four jets. The second highest jet spread is that of case (*a*) where two out of four jets are synchronized. Case (*b*) with none of the four jets synchronized has the lowest jet spread.

The integrated mass-flux ratio obtained from detailed flow-field data at several axial stations is shown in figure 10. The mass-flux ratio is represented as $\dot{m}/\dot{m}_0$ where $\dot{m}$ and $\dot{m}_0$ refer to the mass flux at any station and at the jet exit respectively. In addition to the cases described in figure 9 the single rectangular jet ($M_j = 1.6$) is shown for comparison in figure 10. Trends displayed in figure 10 warrant two comments. First, the visual trend observed in figure 9 (*a–c*) is confirmed and quantified, i.e. the case with all four jets synchronized has the highest entrained mass followed by the case where two of four jets are synchronized, and the completely unsynchronized case has the least entrainment. Second, even the unsynchronized multi-jet case has a higher mass flux than the single rectangular jet.

5. Near-field noise

5.1. *Screech and its harmonics*

Figure 11 compares the screech tone measured at the nozzle lip of one of the jets under conditions of screech synchronization to that obtained from a single rectangular jet. The synchronization does not change the frequency of the screech tone significantly, but it does augment the amplitude. This augmentation is believed to be due to the resonant phase-locking between the screeching jets. The screech Strouhal number ($St(h_j) = fh_j/U_j$) was calculated using the jet's fully expanded narrow dimension (h_j), and the fully expanded jet velocity (U_j). The fully expanded jet dimension (h_j) was determined using a simple geometric relationship given by Tam (1988). The screech tone at a frequency of 6784 Hz ($St(h_j) = 0.128$) stands almost 20 dB over the

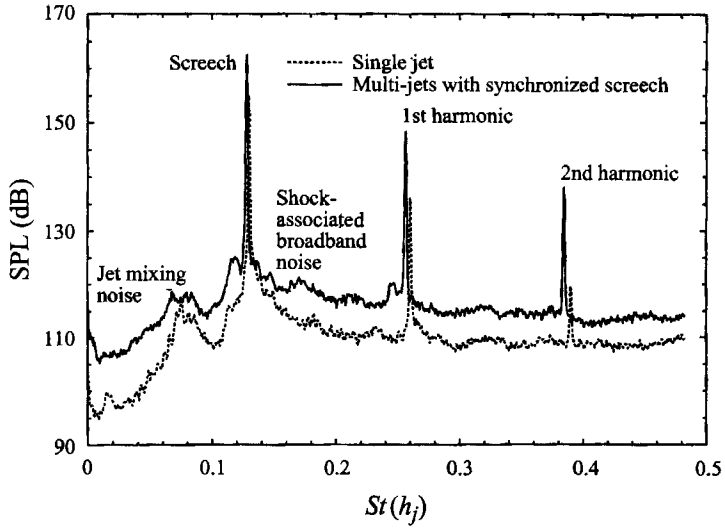

FIGURE 11. Comparison of the sound pressure level spectra of single and multiple screech-synchronized jets.

background level. Two harmonics of the screech tone ($St(h_j) = 0.256$, 0.384) are dominant and also visible in the figure. Note that the noise at all frequencies ranging from 0 to 25600 Hz ($St(h_j) = 0$ to 0.48) is higher for the multi-jet screech-synchronized case than for the single rectangular jet.

Figure 12(*a*, *b*) shows near-field noise contours for the screech tone and its harmonic for the four jets operated at $M_j = 1.6$ under conditions of screech synchronization ($s/h = 8$). The complicated near-field noise map for the fundamental screech tone ($St(h_j) = 0.128$) reveals regions of screech cancellation and reinforcement. These regions are seen as islands of high amplitude (reinforcement) or low amplitude (cancellation). The complex pressure patterns, also observed by Westley & Wooley (1969), appear to be due to the formation of a standing wave, which can be formed in more than one way. In the very near field of the jet (the region dominated by the potential field of the hydrodynamic disturbances in the jet), the standing wave could result from a superposition of the upstream-propagating screech wave and the hydrodynamic pressure fluctuations associated with the downstream-propagating large-scale coherent structures in the jet. As stated earlier, we had avoided the region dominated by hydrodymamic disturbances. However, the complex pressure patterns existed even when one moved away from the very near field of the jet. It appears that reflection of the upstream-propagating screech wave from a nozzle or plenum flange could be responsible for the standing wave pattern observed in this region.

In contrast to the fundamental screech tone, the harmonic propagates in a direction normal to the flow (Powell 1953; Norum 1983). Therefore, the harmonic is not capable of setting up such a standing wave pattern. Consequently, despite its wavelength being shorter than the fundamental screech tone, the near-field pressure map for the harmonic is not as complex (figure 12*b*).

5.2. *Jet and shock-associated broadband noise*

The jet mixing and shock-associated broadband noise bands had centre frequencies at $St(h_j) = 0.075$, and 0.189 respectively. The lower upper band $St(h_j)$ limits for the two bands were 0.066–0.084 and 0.168–0.212 respectively. The upper and lower band limits

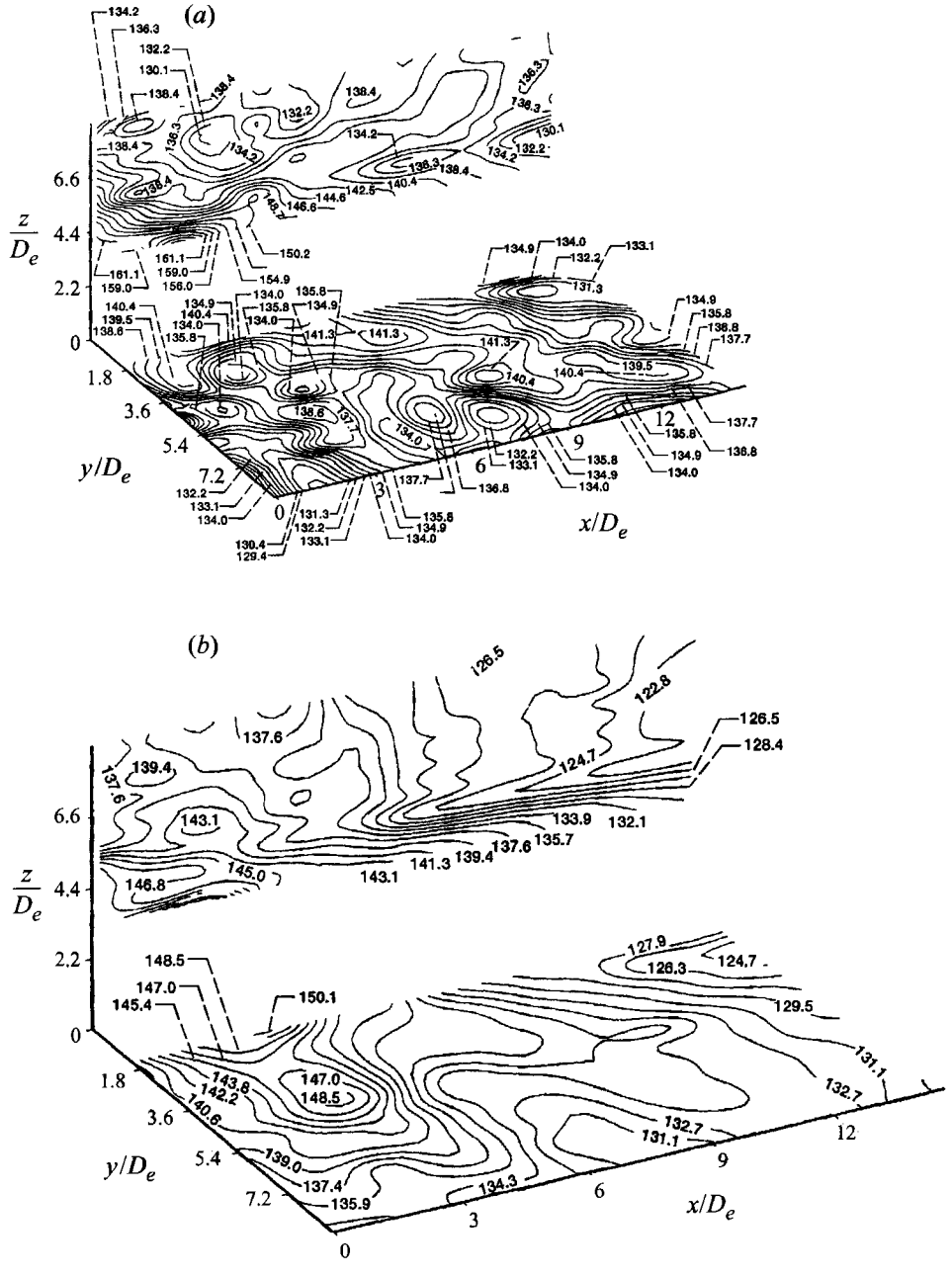

FIGURE 12. Near-field noise map of coherent sound pressure levels. (*a*) Sound pressure levels coherent at the screech frequency. (*b*) Sound pressure levels coherent at the harmonic of the screech frequency.

for $St(h_j)$ are related by $St(h_j)_{upper}/St(h_j)_{lower} = 2^K$ where $K = 1/3$ (one-third octave). The centre band $St(h_j)$ is given by $St(h_j)_{center} = [St(h_j)_{lower}\, St(h_j)_{upper}]^{1/2}$.

It is of interest here to study the noise produced by the multi-jet interaction. To do this we measured the noise in the (X, Y)- and (X, Z)-planes for the screech-synchronized case as well as the case when the four jets were operated individually. Data for the latter case were obtained as follows. The (X, Y)-plane $(z/h = 0)$ was

located midway between jets 2 and 3 (see figure 4*b*). The (X, Z)-plane ($y/h = 0$) was located above the four jets. For the (X, Y)-plane, we took two sets of measurements by operating the top two jets (jets 1 and 2 of figure 2) individually. The noise levels were summed, and 3 dB was added for the contribution of the bottom two jets. For the (X, Z)-plane, four sets of measurements were made by running each jet individually; then the noise levels were summed.

The discussion will focus on the differences between running the jets simultaneously under conditions of screech synchronization and running each jet individually and summing the noise contributions. The sound pressure levels (SPL(dB)) were calculated using $\mathrm{SPL(dB)} = 10\log(p/p_{re})^2$, where p is the r.m.s. sound pressure and p_{re} is the reference r.m.s. sound pressure (20 μPa). The mean-square values of the sound pressure from the four jets operated individually were combined algebraically, assuming that the non-tonal sound sources have a random phase relationship. Hence

$$\frac{p_1^2+p_2^2+p_3^2+p_4^4}{p_{re}^2} = \sum_{i=1}^{4} \mathrm{antilog}\left(\frac{\mathrm{SPL}_i}{10}\right). \tag{5}$$

After algebraic manipulation, the total sound pressure level (SPL_t) can be represented as

$$\mathrm{SPL}_t\mathrm{(dB)} = 10\log\left(\sum_{i=1}^{4} 10^{(\mathrm{SPL}_i/10)}\right). \tag{6}$$

Note that such a summation is not valid for screech tones since the sources do not have a random-phase relationship, and cancellation or reinforcement of sound levels could result. The two bands defined earlier are represented by figures 13 and 14. Parts (*a*) and (*c*) represent the (X, Y)- and (X, Z)-planes for the multi-jet synchronized screech case, whereas parts (*b*) and (*d*) represent the same planes for the sum of jets run individually. For brevity the screech-synchronized multi-jet case and the sum of four jets run individually case will be referred to as case I and case II respectively. Note that unless otherwise stated all directivity angles are measured from the apparent noise source with respect to the flow (downstream) direction.

The jet mixing noise (figure 13*a–d*) which is of prime concern, is higher for case I than for case II in the (X, Y)-plane. However, the peak jet noise source is moved upstream by $2D_e$ for case I as compared to case II. On the (X, Z)-plane case I is actually quieter than case II by 2.3 dB: an observation that could be due to fluid shielding effects in the direction in which the jets are stacked. For the jet mixing noise the directivity angles of the dominant lobes are 50° and 42° for cases I and II respectively in the (X, Y)-plane and 54° and 40° for cases I and II respectively in the (XZ)-plane. Here, let us note that for a single jet at $M_j = 1.6$ (convective Mach number, $M_c = 1.12$ assuming a phase velocity, $c/U_j = 0.7$) the dominant direction of noise radiation as described by Ffowcs Williams (1963) for an ideally expanded supersonic jet is $\theta = \arccos(1/M_c) = 28°$; however, θ was defined differently, as the directivity angle from the nozzle exit with respect to the flow direction. If we convert our measured directivity angles to the convention used by Ffowcs Williams (1963), the directivity angles for the dominant lobes would be 35° and 28° for cases I and II respectively in both planes. Note that the angles for case II match the Ffowcs Williams (1963) prediction. Recall here that, of the various noise components, the jet mixing noise is most important since it has a downstream directivity and is therefore the most difficulty to attenuate. The upstream shift in the peak jet noise source and the larger directivity angles caused by

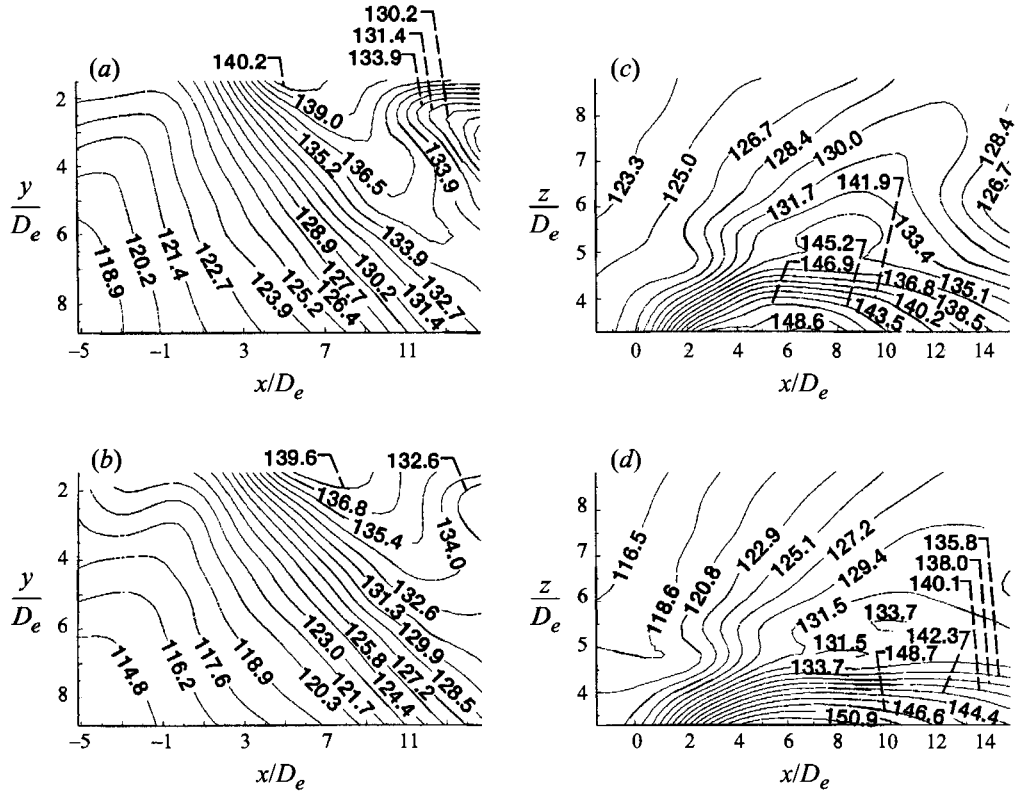

FIGURE 13. Near-field map of the jet mixing noise; third-octave band centred at $St(h_j) = 0.075$ with lower and upper band limits of $St(h_j) = 0.066$ and 0.084 respectively. (*a*) (X, Y)-plane, $z/D_e = 0$, multi-jets with synchronized screech; (*b*) (X, Y)-plane, $z/D_e = 0$, sum of four jets run individually; (*c*) (X, Z)-plane, $y/D_e = 0$, multi-jets with synchronized screech; (*d*) (X, Z)-plane, $y/D_e = 0$, sum of four jets run individually.

the resonant jet interaction are advantageous for noise reduction since the noise could now be suppressed by an acoustically lined ejector of a shorter length.

The shock-associated broadband noise (figure 14*a–d*) shows some very interesting characteristics due to the presence of a dominant lobe directed upstream and a weaker lobe directed downstream. The peak noise levels are 142 and 138 dB for cases I and II in the (X, Y)-plane with no appreciable change in the location of the apparent source. In the (X, Y)-plane both cases display a dual-lobe. The downstream-directed lobe has a directivity angle of 60° to the flow direction. In contrast, the upstream-propagating lobe is directed at 125° to the flow direction for case I and 115° for case II. The peak noise levels in the (X, Z)-plane are 147 and 149 dB for cases I and II respectively. There is an upstream shift in the apparent source for case I on the (X, Z)-plane by $2D_e$. The directivity of the primary (upstream-propagating) noise lobe in the (X, Z)-plane is the same for both cases. The synchronization of jets (case I) is seen to eliminate the downstream-propagating lobe observed in case II. The reason for the disappearance of the secondary (downstream-propagating) lobe remains unknown at this time.

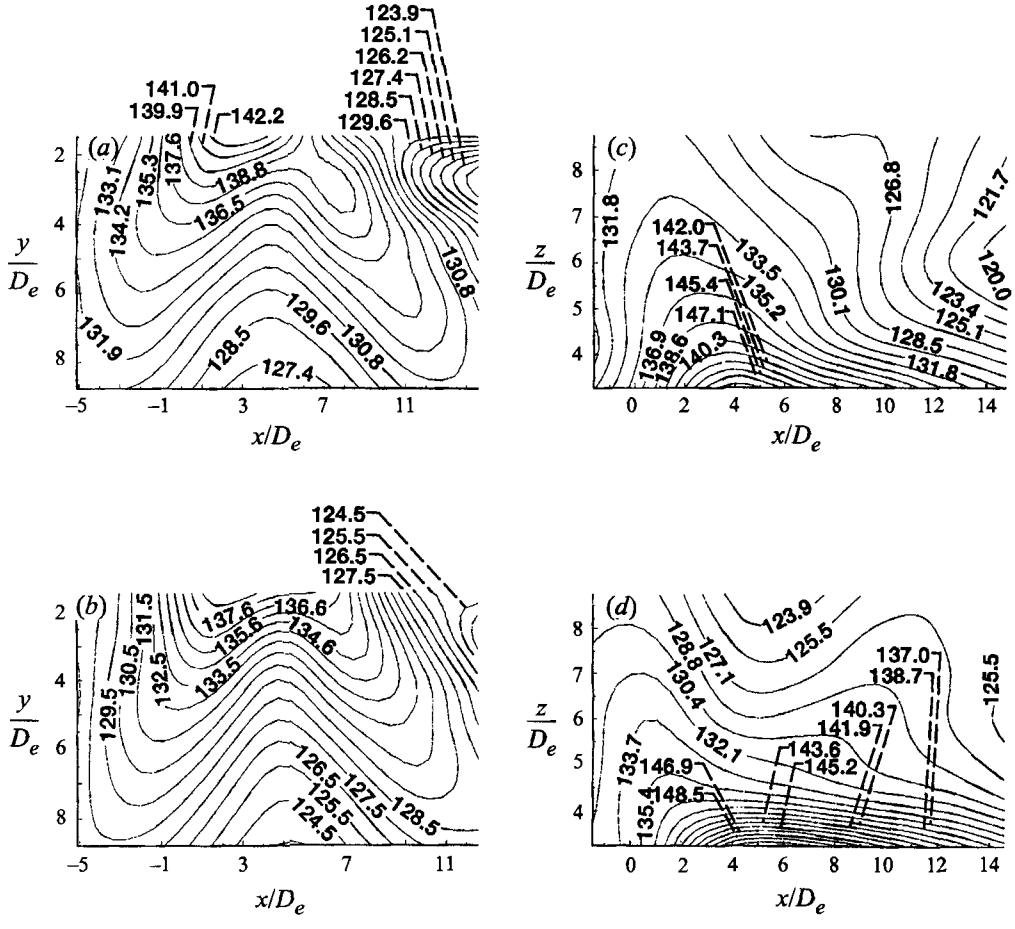

FIGURE 14. Near-field map of the shock-associated broadband noise; third-octave band centred at $St(h_j) = 0.189$ with lower and upper band limits of $St(h_j) = 0.168$ and 0.212 respectively. For a description of parts (*a*)–(*d*) see caption for figure 13.

6. Concluding remarks

We have examined some of the flow and acoustic features of multiple supersonic rectangular jets with phase-locked screech. The primary motivation for this work was the expectation that multi-jets with synchronized screech could provide significant mixing and noise benefits. The secondary motivation was the lack of available information on the aeroacoustics of simple multi-element jet flows.

Using the measured phase of the screech tone in the near field of a single jet, we documented the experimental spacing required for screech synchronization for various jet Mach numbers. A theory that assumed that the phase-locking occurred by a screech source–jet lip interaction between neighbouring jets modelled our experimental data well. Based on the single-jet experiments and theory, we conducted a novel experiment in which the screech instability mode of four supersonic jets was phase-locked. We observed that screech synchronization produced a higher mass flux, moved the peak jet noise source upstream, and caused the jet to radiate noise at larger angles to the flow.

This novel experimental study has achieved our defined goals. We have demonstrated that it is possible to operate four supersonic shock-containing jets with phase-locked

screech and produce both mixing and noise benefits. Finally, we believe that the data are of significant scientific and engineering value in the quest to understand and control multiple, complex supersonic shock-containing jet flows.

The work described in this paper was carried out at the NASA Lewis Research Center, Cleveland, OH. The authors are grateful to Dr E. J. Rice for his ideas and for the development of the multi-jet apparatus. We also thank Dr C. K. W. Tam, Dr J. Bridges, and Dr E. Envia for their technical input. In addition we thank Mr John Abbott, Dr K. Zaman, and Dr R. Mankbadi for their support and encouragement. Finally, Dr J. Panda's help with the schlieren photography and Dr R. Ziegfeld's careful reading of several versions of the manuscript and his suggestions for improving the presentation are highly appreciated.

REFERENCES

BRIDGES, J. & HUSSAIN, F. 1992 Direct evaluation of aeroacoustic theory in a jet. *J. Fluid Mech.* **240**, 469–501.

CHANDRASHEKARA, M. S., KROTHAPALLI, A. & BAGANOFF, D. 1984 Mixing characteristics of an underexpanded multiple jet ejector. *JIAA TR-55, Stanford Univ. Rep., Dept of Aero. & Astro.*

CRIGHTON, D. G. 1974 Mechanisms of excess jet noise. Noise mechanisms, *AGARD-CP-131*, pp. 14–1, 14–7,

CRIGHTON, D. G. 1981 Acoustics as a branch of fluid mechanics. *J. Fluid Mech.* **106**, 261–298.

CRIGHTON, D. G. 1992 The edge-tone feedback cycle; linear theory for the operating stages. *J. Fluid Mech.* **234**, 361–391.

DAVIES, M. G. & OLDFIELD, D. E. S. 1962*a* Tones from a choked axisymmetric jet. I. Cell structure, eddy velocity and source locations. *Acustica* **12**, 257–266.

DAVIES, M. G. & OLDFIELD, D. E. S. 1962*b* Tones from a choked axisymmetric jet. II. The self excited loop and mode of oscillation. *Acustica* **12**, 267–277.

FFOWCS WILLIAMS, J. E. 1963 The noise from turbulence convected at high speed. *Phil. Trans. R. Soc. Lond.* A **255**, 469–503.

FFOWCS WILLIAMS, J. E. & KEMPTON, A. J. 1978 The noise from the large-scale structure of a jet. *J. Fluid Mech.* **84**, 673–694.

GLASS, D. R. 1968 Effects of acoustic feedback on the spread and decay of supersonic jets. *AIAA J.* **6**, 1890–1897.

GUTMARK, E., SCHADOW, K. C. & BICKER, C. J. 1990 Near acoustic field and shock structure of rectangular supersonic jets. *AIAA J.* **28**, 1163–1170.

HAMMITT, A. G. 1961 The oscillation and noise of an overpressure sonic jet. *J. Aerospace Sci.* **8**, 673–680.

KANTOLA, R. A. 1981 Acoustic properties of heated twin jets. *J. Sound Vib.* **79**, 79–106.

KARAMCHETI, K., BAUER, A., SHIELDS, W. L., STEGEN, G. & WOOLLEY, P. J. 1969 Some features of an edge tone flowfield. *NASA SP* 207.

KROTHAPALLI, A., BAGANOFF, D. & KARAMCHETI, K. 1979 An experimental study of multiple jet mixing. *JIAA TR-23, Stanford Univ. Rep. Dept of Aero. & Astro.*

KROTHAPALLI, A., HSIA, Y., BAGANOFF, D. & KARAMCHETI, K. 1986 The role of screech tones in the mixing of an underexpanded rectangular jet. *J. Sound Vib.* **106**, 119–143.

KROTHAPALLI, A., KARAMCHETI, K., HSIA, Y. & BAGANOFF, D. 1983 Edge tones in high-speed flows and their applications to multiple-jet mixing. *AIAA J.* **21**, 937–938.

LASSITER, L. W. & HUBBARD, H. H. 1954 The near noise field of static jets and some model studies of devices for noise reduction. *NACA TN* 3187.

LIGHTHILL, M. J. 1952 On sound generated aerodynamically. I. General theory. *Proc. R. Soc. Lond.* A **211**, 564–587.

LIGHTHILL, M. J. 1954 On sound generated aerodynamically. II. Turbulence as a source of sound. *Proc. R. Soc. Lond.* A **222**, 1–32.

LILLEY, G. M. 1991 Jet noise classical theory and experiments, aeroacoustics of flight vehicles, theory and practice, Vol. 1: noise sources. *NASA RP*-1258; *WRDC, TR*-90-3052 (ed. H. H. Hubbard), pp. 211–289.

LUSH, P. A. 1971 Measurements of subsonic jet noise and comparison with theory. *J. Fluid Mech.* **46**, 477–500.

MANKBADI, R. R. & LIU, J. T. C. 1984 Sound generated aerodynamically revisited: large-scale structures in a turbulent jet as a source of sound. *Phil. Trans. R. Soc. Lond.* A **311**, 183.

MARSTERS, G. F. 1980 Measurements in the flowfield of a linear array of rectangular nozzles. *J. Aircraft* **17**, 774–780.

MOORE, C. J. 1977 The role of shear-layer instability waves in jet exhaust noise. *J. Fluid Mech.* **80**, 321–367.

MORRIS, P. J. 1990 Instability waves in twin supersonic jets. *J. Fluid Mech.* **220**, 293–307.

NORUM, T. D. 1983 Screech suppression in supersonic jets. *AIAA J.* **21**, 235–240.

NORUM, T. D. & SEINER, J. M. 1982 Measurements of mean static pressure and far field acoustics of shock containing supersonic jets. *NASA TM* 84521.

PINCKNEY, S. Z. 1975 A short static-pressure probe design for supersonic flow. *NASA TN-D* 7978.

POLDERVAART, L. J., VINK, A. T. & WIJNANDS, A. P. J. 1968 The photographic evidence of the feedback loop of a two dimensional screeching supersonic jet of air. *6th Intl Cong. on Acoustics, Tokyo, Japan*, pp. F101–104.

POLDERVAART, L. J., WIJNANDS, A. P. J. & BRONKHURST, L. 1973 Aerosonic games with the aid of control elements and externally generated pulses. *AGARD CP*-313, (20) 1–4.

POWELL, A. 1953 On the noise emanating from a two dimensional jet above the critical pressure. *Aero. Q.* **4**, 103–122.

POWELL, A. 1961 On the edgetone. *J. Acoust. Soc. Am.* **33**, 395–409.

RAMAN, G. & RICE, E. J. 1994 Instability modes excited by natural speech tones in a supersonic rectangular jet. *Phys. Fluids* **6**, 3999–4008.

RAMAN, G. & RICE, E. J. 1995 Supersonic jet mixing enhancement using impingement tones from obstacles of various geometries. *AIAA J.* **33**, 454–462.

RAMAN, G. & TAGHAVI, R. 1995 Resonant interaction of a linear array of supersonic rectangular jets: an experimental study. *AIAA Paper* 95-0510 (also *NASA CR* 195398).

RICE, E. J. & RAMAN, G. 1993 Enhanced mixing of a rectangular supersonic jet by natural and induced screech. *AIAA Paper* 93-3263.

ROCKWELL, D. 1983 Oscillations of impinging shear layers. *AIAA J.* **21**, 645–664.

SEINER, J. M., MANNING, J. C. & PONTON, M. K. 1988 Dynamic pressure loads associated with twin supersonic plume resonance. *AIAA J.* **26**, 954–960.

TAGHAVI, R. & RAMAN, G. 1994 Enhanced mixing of multiple supersonic rectangular jets by synchronized screech. *AIAA J.* **32**, 2477–2480.

TAM, C. K. W., SEINER, J. M. & YU, J. C. 1986 Proposed relationship between broadband shock associated noise and screech tones. *J. Sound Vib.* **110**, 309–321.

TAM, C. K. W. 1988 The shock-cell structures and screech tone frequencies of rectangular and non-axisymmetric supersonic jets. *J. Sound Vib.* **121**, 135–147.

TAM, C. K. W. 1991 Jet noise generated by large-scale coherent motion, aeroacoustics of flight vehicles: theory and practice, Vol. 1: noise sources. *NASA RP*-1258; *WRDC TR*-90-3052, (ed. H. H. Hubbard), pp. 311–390.

TAM, C. K. W. 1995 Supersonic jet noise. *Ann. Rev. Fluid Mech.* **27**, 17–43.

WESTLEY, R. & WOOLLEY, J. H. 1969 The near field sound pressures of a choked jet during a screech cycle. Aircraft engine noise and sonic boom. *AGARD CP* 42, pp. 23-1–23-13.

WLEZIEN, R. W. 1989 Nozzle geometry effects on supersonic jet interaction. *AIAA J.* **27**, 1361–1367.